

Document downloaded from:

<http://hdl.handle.net/10251/155011>

This paper must be cited as:

Jurca, B.; Bucur, C.; Primo Arnau, AM.; Concepción Heydorn, P.; Parvulescu, VI.; García Gómez, H. (2019). N-Doped Defective Graphene from Biomass as Catalyst for CO<sub>2</sub> Hydrogenation to Methane. *ChemCatChem*. 11(3):985-990.  
<https://doi.org/10.1002/cctc.201801984>



The final publication is available at

<https://doi.org/10.1002/cctc.201801984>

Copyright John Wiley & Sons

#### Additional Information

This is the peer reviewed version of the following article: B. Jurca, C. Bucur, A. Primo, P. Concepción, V. I. Parvulescu, H. García, *ChemCatChem* 2019, 11, 985, which has been published in final form at <https://doi.org/10.1002/cctc.201801984>. This article may be used for non-commercial purposes in accordance with Wiley Terms and Conditions for Self-Archiving.

# N-Doped Defective Graphene from Biomass as Catalyst for CO<sub>2</sub> Hydrogenation to Methane

Bogdan Jurca<sup>[a]</sup>, Cristina Bucur<sup>[b]</sup>, Ana Primo<sup>[c]</sup>, Patricia Concepción<sup>[c]</sup>, Vasile I. Parvulescu<sup>\*[a]</sup> and Hermenegildo García<sup>\*[c]</sup>

**Abstract:** N-doped, defective graphene obtained by pyrolysis of chitosan at 900°C under Ar exhibits catalytic activity for the Sabatier hydrogenation of CO<sub>2</sub> to CH<sub>4</sub> at temperatures about 500°C with estimated turnover frequencies and activation energy values of 73.17 s<sup>-1</sup> and 24.3 kcal×mol<sup>-1</sup>, respectively. It has been found that this enhanced catalytic activity compared to other related doped defective graphenes derives from the presence of pyridinic N atoms that adsorb CO<sub>2</sub> forming carbamate-type adsorbates.

In the context of diminishing atmospheric CO<sub>2</sub> emissions and implementing low carbon economy, there is a considerable interest in developing large scale processes based on CO<sub>2</sub> as feedstock.<sup>[1]</sup> In spite of the high thermodynamic stability of CO<sub>2</sub> that makes energetically uphill most of its reactions, CO<sub>2</sub> hydrogenations are one of the few exothermic reactions.<sup>[2]</sup> Specifically, the Sabatier reaction converts CO<sub>2</sub> to methane.<sup>[3]</sup> Although there are strategies to perform CO<sub>2</sub> hydrogenation at room temperature under ambient pressure by electrochemical and photochemical techniques,<sup>[4]</sup> the reaction rates and CO<sub>2</sub> conversions under these conditions are unsatisfactorily low. In order to achieve very high conversion rates, catalytically processes are carried out generally at temperatures above 500°C in the presence of metallic catalysts.<sup>[5]</sup>

One of the current lines of research in catalysis is to develop renewable catalysts alternative to those based on metals.<sup>[6]</sup> In this regard, there is much current interest in exploiting the use of carbon materials as metal-free catalysts,<sup>[7]</sup> graphene being one of the preferred metal-free materials for this purpose. Among the various features of graphene with relevance in catalysis, such as large specific surface area, accessibility of active sites, high adsorption capacity, one important advantage of graphene is the possibility to engineer active sites on the sheet either by doping or by other means.<sup>[7b,8]</sup> One of the main advantages of the use of

carbon-based catalysts is that, when obtained from biomass wastes, these materials can be considered as a sustainable and they represent an example of circular economy and waste valorization.<sup>[9]</sup> Implementation of these catalysts in industrial processes will be a step forward moving away from the massive use of metals in catalysis.

In several recent contributions it has been shown that defective graphenes in the absence of metals can promote liquid phase alkene hydrogenation,<sup>[10]</sup> selective gas-phase hydrogenation of acetylene in the presence of a large ethylene excess<sup>[10]</sup> and hydrogenation of nitro groups.<sup>[11]</sup> Since hydrogenations is a reaction class emblematic of transition metal catalysis, it is important to expand further the use of graphenes as heterogeneous catalysts in this type of reactions.

Continuing with this line of research, herein we report the activity of a series of defective graphenes as metal-free catalysts for the Sabatier methanation of CO<sub>2</sub>. Although graphenes have been reported to exhibiting catalytic hydrogenation activity for alkenes, it is important if they are also able to promote hydrogenation of more stable molecules, such as CO<sub>2</sub>, determining their activity and product selectivity. In a recent precedent, it has been found that N-doped graphene quantum dots are catalytically active for CO<sub>2</sub> hydrogenation to CO or CH<sub>4</sub> due to the presence of pyridinic N atoms at the periphery of the dots.<sup>[7d]</sup> The present study reaches similar conclusions, but shows that nanometric dimensions is not a prerequisite and that larger micrometric defective graphene (dG) sheets, even with other dopant heteroatoms, exhibit similar behavior as CO<sub>2</sub> methanation catalyst.

For the present study a series of defective graphenes obtained by pyrolysis of natural polysaccharides from biomass were prepared. The samples of defective graphenes, the corresponding precursors and relevant analytical data are listed in Table 1. Alginate pyrolysis at 900°C under Ar is known to render a dG containing a residual amount of oxygen remaining from the polysaccharide composition. B- and P-doped graphenes (B-dG and P-dG, respectively) were obtained by submitting to pyrolysis the corresponding borate and phosphate esters of alginic acid. N-doped, defective graphene (N-dG) was obtained starting from chitosan that was submitted to pyrolysis also at 900°C. In this case, natural chitosan acts as a simultaneous source of C and N in the final material. All the defective graphenes used in the present study as catalysts have been already reported and there are in the literature extensive characterization data, the appropriate references being included in Table 1. Of note is the fact that none of the defective graphenes used has been prepared using any metal that could contaminate the defective graphenes and that chemical analysis of these samples has shown that the metal content of these defective graphenes are in the ppm level.

[a] PhD Bogdan Jurca and Prof. Vasile I. Parvulescu  
Department of Organic Chemistry, Biochemistry and Catalysis,  
Faculty of Chemistry, University of Bucharest, Bdul Regina  
Elisabeta 4-12, Bucharest 030016, Romania  
E-mail: vasile.parvulescu@chimie.unibuc.ro; bjurca@gw-  
chimie.math.unibuc.ro

[b] PhD Cristina Bucur  
National Institute of Materials Physics, Department of Surfaces and  
Interfaces, Atomistilor 405 A, 077125 Magurele-Ifov, Romania  
E-mail: cristina.bucur@infim.ro

[c] Ana Primo, Patricia Concepción and Prof. Hermenegildo García  
Instituto Universitario de Tecnología Química Consejo Superior de  
Investigaciones Científicas-Universitat Politècnica de Valencia,  
Universitat Politècnica de Valencia, Av. De los Naranjos s/n, 46022  
Valencia, Spain  
E-mail: hgarcia@qim.upv.es

## COMMUNICATION

This contrast with some samples of reduced graphene oxide whose preparation requires the use of an excess of oxidizing reagent, typically  $\text{MnO}_4^-$ , that is retained later in the material in some proportion.<sup>[12]</sup> Also worth noting is the fact that the pyrolytic procedure at 900 °C for preparation of these doped defective graphene samples make them stable at temperatures in the range from 300 to 500 °C that will be used in the catalytic study.

The available characterization data of the materials used in the present study are in good accordance with the reported values. Figure 1 presents selected Raman spectra, a representative transmission electron microscopy (TEM) image and X-ray photoelectron spectroscopy (XPS) peaks to illustrate the data of the most active N-dG sample under study. Briefly, Raman spectra show the presence of the G and D bands appearing at about 1600 and 1350  $\text{cm}^{-1}$ , indicating the presence of defects corresponding to oxygenated functional groups, dopant elements and the presence of carbon vacancies on the sheet. TEM images show the characteristic morphology of the sheets with the light contrast expected for single or few-layers graphenes. XPS shows the C1s peak that can be deconvoluted as graphenic carbon in a percentage of 80 % or above and carbon atoms bonded to oxygen or heteroatoms in lesser proportions. Besides oxygen that was present in all the dG samples, the corresponding heteroatom expected depending on the sample was also detected. In each case the peak corresponding to the heteroatom could be fitted to two components.

**Table 1.** Defective graphenes studied as Sabatier catalysts with indication of their origin, analytical data and appropriate literature reference.

Sample	Precursor	C (at. %) <sup>[a]</sup>	X (at. %) <sup>[a]</sup>	Ref.
dG	Alginate	(C=C) 89.1 (C=O) 10.9	--	[13a]
B-dG	Alginic Borate	(C=C) 86.2 (C=O) 12.4	(BC <sub>3</sub> ) 0.35 (BCO <sub>2</sub> ) 0.83	[13b]
P-dG	Alginic Phosphate	(C=C) 58.4 (C=P) 37.2 (C=O) 0.28	(PC <sub>3</sub> ) 1.7 (PCO <sub>2</sub> ) 2.4	[13c]
N-dG	Chitosan	(C=C) 82.9 (C=N) 12.9	(NC <sub>3</sub> ) 3.5 (NC <sub>2</sub> ) 0.6	[13a]

[a] at. % refers to the atomic percentage determined from XPS measurements.

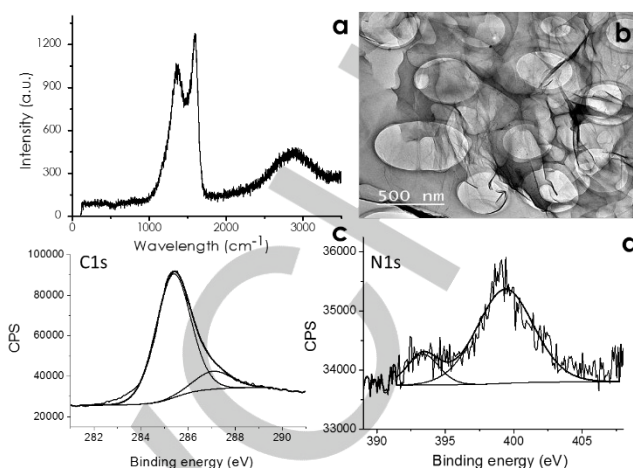


**Figure 1.** a) Raman spectrum upon 514 nm excitation of N-dG; b) a representative TEM image of N-dG; c and d) XPS C1s and N1s peaks of N-dG and the best deconvolution to individual components. These data are in agreement with those reported previously in the literature for this material.<sup>[9]</sup>

In the case of B1s the two components have binding energies indicating BCCC and BCOO environment. The P2p peak exhibits two different families that correspond to PCCC and PCOO. In the case of N doping, four different populations of N atoms similar to pyridinic, pyrrolic, graphitic and N-oxide types of N atoms were determined. Table 1 contains the analytical data for the elements of the defective graphene samples and their distribution among the various coordination environments, while Figures S1 and S3 in the supporting information presents XPS C1s, O1s and the corresponding heteroatom peaks for the series of samples under study.

The samples of defective graphenes were used as catalysts for the gas-phase hydrogenation of  $\text{CO}_2$  at 10 bar pressure in the range of temperatures from 300 to 500 °C. Blank controls showed that negligible conversions for temperatures of 400 °C or below, while  $\text{CO}_2$  conversion in the absence of any catalyst at 450 and 500 °C was 1.9 and 6.0 %, respectively. Similarly, a blank experiment exposing N-dG to  $\text{H}_2$  at 500 °C in the absence of  $\text{CO}_2$  indicates the formation of detectable, but negligible, amounts of  $\text{CH}_4$  (less than 1 %), much below the amounts formed when  $\text{CO}_2$  is present. This control experiment indicates that  $\text{CO}_2$  is the origin of the  $\text{CH}_4$  formed in the hydrogenation.

All the defective graphene samples exhibited some catalytic activity, the predominant product being  $\text{CH}_4$ , accompanied in some cases with a minor amount of CO. The percentage of CO grows in general terms with the reaction temperature. Nevertheless, the selectivity to CO was below 1 % for three catalysts in every condition, except for B-dG that was somewhat higher, reaching in one case over 3 % CO selectivity. A summary of the activity data are presented in Table 2. Mass balances and selectivity values were calculated assuming that the product detected are the only products formed.

As expected the  $\text{CO}_2$  conversion increases with the temperature, being the highest at 500 °C. The best performing defective graphene was the N-doped. For N-dG, increasing the

amount of catalyst increases proportionally CO<sub>2</sub> conversion, reaching under the optimal operating conditions a conversion over 50 %. To check stability of N-dG, a continuous flow experiment in which the sample was submitted to treatment for an extended time in which the temperature of the reactor was increased in 50°C increments from 300 to 500°C, each step lasting 1 h and then, gradually decreased by 50°C decrements each hour and the cycle repeated subsequently showed no changes in the catalytic activity for each of the temperature steps in the total 20 h of the experiment. This activity data indicates the catalytic stability of N-dG. Under the best conditions at 500°C, a turnover frequency of 73.17 s<sup>-1</sup> was determined considering the pyridinic N atoms present in N-dG as the active sites (see below). It is important to note that the total amount of CH<sub>4</sub> formed in this long run experiment (higher than 10 mmols) is over one order the magnitude the total amount of C present in N-dG (about 1 mmol) in case of complete decomposition, what clearly does not happen. N-dG catalyst stability together with the amount of CH<sub>4</sub> formed indicates that CO<sub>2</sub> is the origin of the CH<sub>4</sub> formed. From the dependence of the conversion with the temperature in the range from 300 to 500°C, an activation energy of 24.3 kcal×mol<sup>-1</sup> was estimated (see Figure S4 in supporting information).

To assess the possible changes occurring to N-dG under the reaction conditions, the sample submitted to extended catalytic evaluation (20 h) was analysed by XPS, observing the occurrence of partial oxidation in the used sample respect to the corresponding spectra of the fresh N-dG sample. Thus, XPS of the used N-dG exhibits an increase in the O/C ratio and a shift of the C1s peaks towards higher binding energy (see supporting information, Figures S1-S3, Tables S1-S3). Partial oxidation of surface of metallic catalysts under CO<sub>2</sub> hydrogenation conditions is a well-established fact,<sup>[5b,c]</sup> and a similar surface restructuring seems to occur also in the case of N-dG, increasing the amount or oxygen in the used N-dG sample. These oxygen atoms come from the splitting of CO<sub>2</sub> on the surface of N-dG. According to XPS, the fresh sample has five oxygen families while the spent N-dG has only three types, although they are common in both samples. The fact that the used N-dG sample has only three components, instead of five, indicates the preferential increase of these three types of oxygen, making the other two oxygen families present in the fresh sample negligible. However, the N1s peak of used N-dG remains mostly unchanged under reaction conditions, increasing slightly in intensity respect to C under the reaction conditions, and showing the presence of four

**Table 2.** Conversion and selectivity for the Sabatier methanation catalysed by a series of defective graphenes. Reaction conditions: pressure 10 bar, flow rates: H<sub>2</sub>: 3 mL×min<sup>-1</sup>; CO<sub>2</sub>: 1 mL×min<sup>-1</sup>.

Defective Graphene	Temperature (°C)	Amount of catalyst (mg)	CO <sub>2</sub> conversion (%)	CH <sub>4</sub> selectivity (%)
B-dG	300; 350	20	0	--
B-dG	400	20	0.5	100
B-dG	450	20	2.2	97.3
B-dG	500	20	6.1	96.8

P-dG	300; 350	20	0	--
P-dG	400	20	0.9	100
P-dG	450	20	2.7	99.5
P-dG	500	20	6.1	99.3
N-dG	300	20	0	--
N-dG	350	20	0.3	100
N-dG	400	20	1.4	100
N-dG	450	20	4.9	99.6
N-dG	500	20	12.9	99.5
N-dG	300	40	0.05	100
N-dG	350	40	0.3	100
N-dG	400	40	1.7	99.2
N-dG	450	40	6	99.5
N-dG	500	40	17.2	99.7
N-dG <sup>[a]</sup>	300	20	1.9	100
N-dG <sup>[a]</sup>	350	20	12.8	100
N-dG <sup>[a]</sup>	400	20	19.7	99.4
N-dG <sup>[a]</sup>	450	20	41.8	99.3
N-dG <sup>[a]</sup>	500	20	52.3	99.2
Empty reactor	300; 350	0	0	--
Empty reactor	400	0	0.3	100
Empty reactor	450	0	1.9	100
Empty reactor	500	0	6	99.5

[a] Pressure 25 bars.

components corresponding to pyridinic (398.2 eV, 28 %), graphenic (399.8 eV, 49 %), pyrrolic (401.0 eV, 10 %) and N-oxide (403.0 eV, 13 %) atoms in the very similar proportion as the fresh N-dG sample. The slight increase of the N/C ratio could indicate some C decomposition, probably as CO<sub>2</sub> or CH<sub>4</sub>, due to the occurrence of some slight oxidation and the minor CH<sub>4</sub> evolution observed in the blank control exposing N-dG to H<sub>2</sub> at 500 °C as commented earlier based on the O/C ratio.

To gain information about the nature of the active sites and the possible role of the dopant N atoms in the hydrogenation, titration of the acid and basic sites of N-dG was done by NH<sub>3</sub> and CO<sub>2</sub> adsorption-desorption measurements. The latter data were particularly relevant considering that the reaction under study involves CO<sub>2</sub> as substrate. It should be reminded that N-dG sample is obtained by pyrolysis at 900 °C and the sample is thermally stable upon heating from 200 to 600 °C without mass loss (see Figure S6 in the supporting information). This thermal stability of N-dG contrasts with some other carbon samples

reported in the literature that release small molecules upon heating, because they were prepared at much lower temperatures between 300 and 500 °C.<sup>[7e]</sup> These adsorption/desorption experiments of CO<sub>2</sub> and NH<sub>3</sub> showed that the acidity of N-dG was very minor compared to its basicity. Table S5 and S6 provides a summary of the most salient values from these titration measurements. It is worth noting that the amount of CO<sub>2</sub> adsorbed determined in the TPD measurement agrees well with the amount of pyridinic N atoms determined from the N content of N-dG (4.7 % and the percentage of pyridinic N of 28 %), assuming a 1-to-1 stoichiometry the CO<sub>2</sub> titration data indicates that most of the pyridinic N atoms are able to adsorb one CO<sub>2</sub> molecule. This fact is in good accordance with the expectations based on molecular chemistry that shows that while pyridine is a base, pyrrole and quaternary N are much less or not basic. These results are also in agreement with the proposal of Wu and coworkers that have suggested pyridinic N atoms at the periphery of graphene dots as the active sites of CO<sub>2</sub> hydrogenation in these materials.<sup>[7d]</sup>

To get experimental evidence in support of the nature of the sites responsible for the interaction of CO<sub>2</sub> with N-dG, vibrational spectroscopy of N-dG before and after adsorption of CO<sub>2</sub> in the absence and presence of H<sub>2</sub> was recorded. Appearance of a band at 1750 cm<sup>-1</sup> after CO<sub>2</sub> adsorption at 400 °C that could be attributable to the CO stretching bands of carbamic acid was observed. This interpretation is in agreement with the formation of carbamic acid upon dissolution of CO<sub>2</sub> into pyridine.<sup>[2c,d]</sup> If, on the other hand, the N-dG samples is heated at 400°C coadsorbing simultaneous CO<sub>2</sub> and H<sub>2</sub> in a ratio 1 to 1 and then recording the IR spectrum at room temperature either through the N-dG catalyst or through the gas phase, besides the band of carbamic acid of somewhat lower intensity than in the absence of H<sub>2</sub>, the IR spectrum of the gas phase detects the formation of CO by monitoring its characteristic peak at 2145 cm<sup>-1</sup>. Of note is that the contact time of the IR measurements is about 30 min. Detection of CO in the gas phase could suggest that this compound is the key intermediate in the CO<sub>2</sub> hydrogenation as it has been previously reported in the case of some metal catalyst. Figure 2 shows a summary of the Raman spectra to illustrate the variations in the vibration bands observed in these measurements.

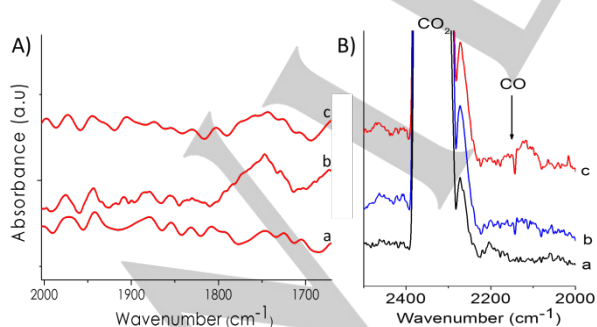


**Figure 2.** A) IR spectra in the N-CO-O range of the fresh sample (a), after CO<sub>2</sub> adsorption (4 mbar) at 400°C (b), and after co-adsorption of CO<sub>2</sub> (4 mbar) and H<sub>2</sub> (4 mbar) at 400°C (c). B) IR spectra of the gas phase in the CO region after CO<sub>2</sub> adsorption (4 mbar) at 25°C (a) and 400°C (b), and after co-adsorption of CO<sub>2</sub> (4 mbar) and H<sub>2</sub> (4 mbar) at 400°C. After CO<sub>2</sub> adsorption and increasing

the temperature to 400°C, a broad IR band at 1750 cm<sup>-1</sup> is recorded which can be related to carbamate (N-CO-O) formation. Noticeably, co-adsorbing CO<sub>2</sub> and H<sub>2</sub>, the band at 1750 cm<sup>-1</sup> on the catalyst surface appears again, but with lesser intensity. Simultaneously in the gas phase a weak band at 2145 cm<sup>-1</sup> associated to the evolution of CO could be detected (see frame B).

All these observations are in agreement with the preferential adsorption of CO<sub>2</sub> as acid on the basic pyridinic N atoms on N-dG that are the most basic sites on N-dG. This favorable CO<sub>2</sub> adsorption will justify the higher catalytic activity of N-dG, respect to other defective graphene, lacking basic sites of similar strength. Precedents in the literature have shown that defective graphenes are able to catalyze hydrogenations by activating molecular hydrogen.<sup>[14]</sup> The active sites for hydrogen activation could be either at carbon vacancies and holes, the periphery of the sheet or at frustrated Lewis acid base pairs, as it has been reported for other hydrogenations reaction promoted by defective graphenes.<sup>[8c,d]</sup>

In conclusion, defective graphenes obtained from biomass wastes and in the absence of metals can promote the selective hydrogenation of CO<sub>2</sub> to methane. The N-doped defective graphene obtained by pyrolysis at 900 °C appears to exhibit significant stability at temperatures below 500 °C under hydrogenation conditions. The catalytic activity of these materials is notably improved by the presence of N atoms as dopant elements. Adsorption measurements indicate that this catalytic activity is related to the basicity introduced in the (N)-dG by pyridinic N atoms and it has been possible by infrared spectroscopy to characterize the carbamate formed in the adsorption. Considering the possibility that graphenes offer to engineer active sites and the possibility to modulate their electronic density and work function, the present results open new avenues in the development of sustainable metal-free catalysts for CO<sub>2</sub> activation.

## Experimental Section

Defective graphene preparation.

Synthesis of defective graphene (dG)

Alginate sodium salt from brown algae (Sigma) was pyrolyzed in argon atmosphere according to the following heating program: 200°C for 2 h to anneal the sample and then heating at 10°C\*min<sup>-1</sup> up to 900°C for 6 h. This multilayer defective graphene powder is sonicated at 700 W during 1 h to obtain the dispersed dG.

Synthesis of defective N-doped graphene (N-dG)

Chitosan from Aldrich (low molecular weight) was pyrolyzed in argon atmosphere using the same heating program indicated for the preparation of dG. This multilayer defective N-doped graphene powder is sonicated at 700 W during 1h to obtain the dispersed N-dG in water. The solid was recovered upon evaporation of H<sub>2</sub>O.

Synthesis of defective B-doped graphene (B-dG)

0.5 g of alginic acid sodium salt from brown algae (Sigma) was dissolved in a boric acid aqueous solution (50 mg of  $\text{H}_3\text{BO}_3$  in 50 ml of water). The solution was filtered with syringe filters of 0.45  $\mu\text{m}$  of diameter pore for removing the impurities present in commercial alginate. Before pyrolysis, the solution was concentrated by heating at 100°C in an oven overnight. The pyrolysis was performed using the same heating program as indicated for the preparation of dG. This multilayer defective B-doped graphene powder is sonicated at 700 W for 1 h to obtain dispersed B-dG in water. The material is recovered by slow evaporation of  $\text{H}_2\text{O}$ .

#### Synthesis of defective P-doped graphene (P-dG)

0.5 g of alginic acid sodium salt from brown algae (Sigma) was dissolved in a sodium phosphate dibasic monohydrate aqueous solution (1.6 g in 50 ml of water). The solution was filtered in a pressure filtration equipment using 0.22  $\mu\text{m}$  pore diameter filters for removing the impurities present in commercial alginate. Before pyrolysis, the solution was concentrated by heating in an oven at 100°C overnight. The pyrolysis was performed using the same oven program as indicated for the preparation of dG. The resulting defective P-doped graphene was sonicated at 700 W during 1 h in water to obtain P-dG dispersed in the reaction mixture.

#### Characterization.

IR spectra were recorded with a Nexus 8700 FTIR spectrometer using a DTGS detector, acquiring at 4  $\text{cm}^{-1}$  resolution. An IR cell allowing in situ treatments in controlled atmospheres and temperatures from 25°C to 500°C was connected to a vacuum system with gas dosing facility. For IR studies the sample was deposited onto a germanium IR transparent wafer and activated in vacuum ( $10^{-5}$  mbar) at 120°C for 1.5 h. After activation the sample was cooled down to 25°C and 4 mbar  $\text{CO}_2$  was adsorbed at 25°C. Then the temperature was increased at 400°C. At that temperature  $\text{H}_2$  (4 mbar) was co-adsorbed. IR spectra of the sample and the gas phase was acquired at each point. XPS measurements were carried out on a SPECS surface-science cluster, including an XPS spectrometer equipped with a monochromatic Al  $\text{K}_{\alpha 1}$  X-ray source (photon energy 1486.74 eV) and operating under ultrahigh vacuum at  $1.3 \times 10^{-13}$  atm. The photoelectrons were collected by a 150 mm radius Phoibos electron analyzer with a pass energy of 30 eV. The binding energies were corrected for the surface-charging effects during the measurements by using the C1s core level (284.5 eV) of the adventitious carbon as an internal reference. Exhaustive chemical analysis of the metal content of dG and (N)-dG showed that no metals are detectable in percentages above the 10 ppm detection limit.

#### $\text{CO}_2$ hydrogenation

Catalytic tests were performed in a setup (Microactivity Reference, PID Eng&Tech) equipped with a stainless steel (316 SS) fixed bed tube reactor (Autoclave Engineers) featured with an inner K-type thermocouple. Two mass flow controllers (EL-FLOW Select, Bronkhorst) were used to feed the mixture of the inlet gases: hydrogen (5.0, Linde) and carbon dioxide (4.5, Linde). The total gas flow rate was checked before each experiment with a burette connected to the outlet of the reactor setup.

The corresponding amount (20 or 40 mg) of catalyst was introduced as powder in the reactor; air was removed by flushing the system at room temperature for 15 min. with 30  $\text{mL} \times \text{min}^{-1}$   $\text{H}_2$  and 10  $\text{mL} \times \text{min}^{-1}$   $\text{CO}_2$ , followed by 10 min. at the flow rates used during the experiments: 3  $\text{mL} \times \text{min}^{-1}$   $\text{H}_2$  and 1  $\text{mL} \times \text{min}^{-1}$   $\text{CO}_2$ . Afterwards, the reactor was pressurized at 10/25 bar. Five reaction temperatures between 300 and 500°C were investigated. For each temperature, a set of three successive GC analyses were performed (at 5, 25 and 45 minutes after the stabilization of the temperature). The values of the  $\text{CO}_2$  conversion obtained from the last two GC measurements coincide very well, indicating that the reactor setup reached the steady state operation conditions.

GC analyses were performed using  $\text{H}_2$  as carrier gas on an Agilent 7890A chromatograph equipped with a capillary PLOT column (RT-MSieve 5A, Restek) and a TCD detector. Temperature program includes a 5 min. dwell at 50°C, a ramp with  $25^\circ\text{C} \times \text{min}^{-1}$  to 250°C followed by a final dwell of 5 min., allowing thus a good separation between  $\text{O}_2$ ,  $\text{N}_2$ ,  $\text{CH}_4$ ,  $\text{CO}$  and  $\text{CO}_2$ . The gas samples were injected through a remotely controlled 6-way valve (A4C6WE, Vici) kept at ambient temperature. The reproducibility of the analysis system was checked prior to each experiment by injecting a series of three successive samples of gas mixture passed through the reactor at room temperature.

#### Conflicts of interest

There are no conflicts to declare.

#### Acknowledgements

Financial support by the Spanish Ministry of Economy and Competitiveness (Severo Ochoa, Grapas and CTQ2015-69153-CO2-R1) and Generalitat Valenciana (Prometeo 2017-083) is gratefully acknowledged. A.P. thanks the Spanish Ministry for a Ramón y Cajal research associate contract. V.I.P. kindly acknowledges UEFISCDI for financial support (projects PN-III-P4-ID-PCE-2016-0146, Nr. 121/2017, PN-III-P4-ID-PCCF-2016-0088 and PN-III-P1-1.2-PCCDI-2017-0541). Cristina Bucur thanks IFTM for the financial support.

**Keywords:** N-doped defective graphene • hydrogenation of  $\text{CO}_2$  to methane • pyridinic active species • carbamate intermediates •

- [1] a) R. A. Van Santen in *Catalysis for Renewables* (Eds.: G. Centi, R. A. Van Santen), Wiley-VCH, Weinheim, **2007**, pp. 1-20; b) M. Aresta in *Carbon Dioxide as Chemical Feedstock* (Eds.: M. Aresta), Wiley-VCH, Weinheim, **2010**, pp. 1-14; c) K. M. K. Yu, I. Curcic, J. Gabriel, S. C. E. Tsang, *ChemSusChem* **2008**, *1*, 893-899.
- [2] a) X. Xiaoding, J. Moulijn, *Energ. Fuel* **1996**, *10*, 305-325; b) T. Sakakura, J. C. Choi, H. Yasuda, *Chem. Rev.* **2007**, *107*, 2365-2387; c) M. Aresta, A. Dibenedetto, E. Quaranta, *Reaction Mechanisms in Carbon Dioxide Conversion*, Springer, **2016**; d) T. Sakakura, J.-C. Choi, H. Yasuda, *Chemical Reviews* **2007**, *107*, 2365-87.
- [3] a) K. P. Brooks, J. Hu, H. Zhu, R. J. Kee, *Chem. Eng. Sci.* **2007**, *62*, 1161-1170; b) S. K. Hoekman, A. Broch, C. Robbins, R. Purcell, *Int. J. Greenh. Gas Con.* **2010**, *4*, 44-50; c) S. Roensch, J. Schneider, S. Matthischke, M. Schlueter, M. Goetz, J. Lefebvre, P. Prabhakaran, S. Bajohr, *Fuel* **2016**, *166*, 276-296.
- [4] a) B. Obama, *Science* **2017**, *355*, 126-129; b) J. M. Wallace, I. M. Held, D. W. J. Thompson, K. E. Trenberth, J. E. Walsh, *Science* **2014**, *343*, 729-730; c) H. Rao, L. C. Schmidt, J. Bonin, M. Robert, *Nature* **2017**, *548*, 74-77; d) K.-L. Bae, J. Kim, C. K. Lim, K. M. Nam, H. Song, *Nat. Commun.* **2017**, *8*, 1156.
- [5] a) K. Mueller, M. Staedter, F. Rachow, D. Hoffmannbeck, D. Schmeisser, *Environ. Earth Sci.* **2013**, *70*, 3771-3778; b) D. J. Miller, M. C. Biesinger, N. S. McIntyre, *Surface and Interface Analysis* **2002**, *33*, 299-305; c) S. Günther, A. Scheibe, H. Bluhm, M. Haevecker, E. Kleimenov, A. Knop-Gericke, R. Schlögl, R. Imbühl, *J. Phys. Chem. C* **2008**, *112*, 15382-93.
- [6] A. Thomas, A. Fischer, F. Goettmann, M. Antonietti, J.-O. Mueller, R. Schloegl, J. M. Carlsson, *J Mater. Chem.* **2008**, *18*, 4893-4908.
- [7] a) D. R. Dreyer, C. W. Bielawski, *Chem. Sci.* **2011**, *2*, 1233-1240; b) H. Hu, J. H. Xin, H. Hu, X. Wang, Y. Kong, *Appl. Catal. A-Gen.* **2015**, *492*, 1-9; c) S. Navalón, A. Dhakshinamoorthy, M. Alvaro, H. Garcia, *Chem.*

- Rev. **2014**, *114*, 6179-6212; d) J. Wu, C. Wen, X. Zou, J. Jimenez, J. Sun, Y. Xia, M.-T. Fonseca Rodrigues, S. Vinod, J. Zhong, N. Chopra, I. N. Odeh, G. Ding, J. Lauterbach, P. M. Ajayan, *ACS Catalysis* **2017**, *7*, 4497-503; e) K. Friedel Ortega, R. Arrigo, B. Frank, R. Schlögl, A. Trunschke, *Chem. Mater.* **2016**, *28*, 6826-39.
- [8] a) C. K. Chua, M. Pumera, *Chem-Eur. J* **2015**, *21*, 12550-12562; b) X. Duan, H. Sun, Z. Ao, L. Zhou, G. Wang, *Carbon* **2016**, *107*, 371-378; c) D. S. Su, G. Wen, S. Wu, F. Peng, R. Schloegl, *Angew. Chem. Int. Edit.* **2017**, *56*, 936-964; d) S. Navalon, A. Dhakshinamoorthy, M. Alvaro, M. Antonietti, H. Garcia, *Chem. Soc. Rev.* **2017**, *46*, 4501-4529.
- [9] A. Primo, P. Atienzar, E. Sanchez, J. Maria Delgado, H. Garcia, *Chem. Comm.* **2012**, *48*, 9254-9256.
- [10] A. Primo, F. Neatu, M. Florea, V. Parvulescu, H. Garcia, *Nat. Commun.* **2014**, *5*, 5291.
- [11] M.-M. Trandafir, M. Florea, F. Neatu, A. Primo, V. I. Parvulescu, H. Garcia, *ChemSusChem* **2016**, *9*, 1565-1569.
- [12] R. Ye, J. Dong, L. Wang, R. Mendoza-Cruz, Y. Li, P.-F. An, M. J. Yacamán, B. I. Yakobson, D. Chen, J. M. Tour, *Carbon* **2018**, *132*, 623-631.
- [13] a) A. Primo, A. Forneli, A. Corma, H. Garcia, *ChemSusChem* **2012**, *5*, 2207-2214; b) A. Dhakshinamoorthy, A. Primo, P. Concepcion, M. Alvaro, H. Garcia, *Chem-Eur J* **2013**, *19*, 7547-7554; c) M. Latorre - Sánchez, A. Primo, H. Garcia, *Angew. Chem. Int. Edit.* **2013**, *52*, 11813-11816.
- [14] Z. Wei, D. Guo, Y. Hou, H. Xu, Y. Liu, *J Taiwan Inst. Chem. E.* **2016**, *67*, 126-129.

WILEY-VCH

---